Published in final edited form as:
Dev Neurobiol. 2014 March ; 74(3): 351–364. doi:10.1002/dneu.22154.

Axonal cap-dependent translation regulates presynaptic p35

Kuangfu Hsiao,
Department of Neuroscience, Friedman Brain Institute, Icahn School of Medicine and Graduate School of Biomedical Sciences at Mount Sinai, 1470 Madison Avenue, New York, NY 10029

Ozlem Bozdagi, and
[1]Department of Psychiatry, Friedman Brain Institute, Icahn School of Medicine and Graduate School of Biomedical Sciences at Mount Sinai, 1470 Madison Avenue, New York, NY 10029

Deanna L. Benson*
Department of Neuroscience, Friedman Brain Institute, Icahn School of Medicine and Graduate School of Biomedical Sciences at Mount Sinai, 1470 Madison Avenue, New York, NY 10029

Abstract

Axonal growth cones synthesize proteins during development and in response to injury in adult animals. Proteins locally translated in axons are used to generate appropriate responses to guidance cues, contribute to axon growth, and can serve as retrograde messengers. In addition to growth cones, mRNAs and translational machinery are also found along the lengths of axons where synapses form en passant, but contributions of intra-axonal translation to developing synapses are poorly understood. Here, we engineered a subcellular-targeting translational repressor to inhibit mRNA translation in axons, and we used this strategy to investigate presynaptic contributions of cap-dependent protein translation to developing CNS synapses. Our data show that intra-axonal mRNA translation restrains synaptic vesicle recycling pool size and that one target of this regulation is p35, a Cdk5 activating protein. Cdk5/p35 signaling regulates the size of vesicle recycling pools, p35 levels diminish when cap-dependent translation is repressed, and restoring p35 levels rescues vesicle recycling pools from the effects of spatially targeted translation repression. Together our findings show that intra-axonal synthesis of p35 is required for normal vesicle recycling in developing neurons, and that targeted translational repression provides a novel strategy to investigate extrasomal protein synthesis in neurons.

Keywords

targeted repression; cap-dependent translation; Cdk5; mRNA transport; vesicle recycling

INTRODUCTION

Cells have developed elaborate mechanisms to transport proteins to particular destinations. Additionally, cells transport particular mRNAs to distant sites that can be translated close to where the new proteins are needed. Such local protein translation is used as a mechanism to

*To whom correspondence should be addressed: Deanna L. Benson, Icahn School of Medicine at Mount Sinai, Friedman Brain Institute, 1470 Madison Avenue, 9-140, New York, NY 10029.

generate a focal response to a restricted stimulus. In developing neurons, guidance cues and growth factors can stimulate the translation of proteins in axonal growth cones that are used to mediate turning responses, promote growth or serve as retrograde messengers (Campbell and Holt, 2001; Zheng et al., 2001; Brittis et al., 2002; Wu et al., 2005; Leung et al., 2006; Yao et al., 2006; Cox et al., 2008; Kundel et al., 2009; Perry et al., 2012). Outside of growth cones, synthesis in axons is poorly understood (Deglincerti and Jaffrey, 2012). Several studies show that mRNAs and proteins important for protein translation are localized all along the lengths of axons (Bassell et al., 1994; Zheng et al., 2001; Poon et al., 2006; Christie et al., 2009; Merianda et al., 2009; Taylor et al., 2009; Vogelaar et al., 2009; Zivraj et al., 2010; Jung et al., 2012), suggesting that intra-axonal translation may be widespread, but few studies have addressed this directly (Zhang and Poo, 2002; Lyles et al., 2006; Taylor et al., 2013) in large part because the selective manipulation of axons in the presence of postsynaptic targets has proven difficult.

In order to investigate axonal contributions of translation to synapse development, we generated a cap-dependent translation repressor that would be active at sites distal to cell bodies and expressed it small numbers of neurons. This permitted us to selectively analyze effects on axons. Our data show that presynaptic repression of cap-dependent mRNA translation enlarges synaptic vesicle recycling pool size. This effect is due in part to decreased levels of p35, a Cdk5 activating protein (Su and Tsai, 2011). p35 is localized to vesicle release sites, its levels diminish when cap-dependent translation is suppressed, its mRNA is transported to and can be locally synthesized within axons, and cap-*in*dependent synthesis of p35 can rescue vesicle recycling sites from the effects of cap-dependent repression. Together our data support that intra-axonal synthesis of p35 regulates vesicle recycling in developing neurons and that a distally targeted translational repressor can be used to investigate extrasomal protein synthesis in neurons.

METHODS

Neuron Cultures

All procedures involving animals were carried out in accordance with US National Institutes of Health guidelines and were approved by the Animal Care and Use Committee of the Icahn School of Medicine at Mount Sinai. Hippocampi were isolated from embryonic day 18 (E18) rats and plated at 12,000 cells cm^2 on poly-lysine–coated coverslips (PLL; 1 mg/ml; Sigma) alone for growth cone collapse assay or PLL followed by laminin (13 μg/ml; Sigma) for all other assays. Neurons were maintained in Neurobasal Media (Invitrogen) containing NS21 (Chen et al., 2008) in a 5% CO_2, 37°C incubator. Neurons were transfected with Lipofectamine 2000 (Invitrogen) at 9 – 11 DIV as described previously (Burton et al., 2012) and cDNAs were expressed 18 – 24 h before live imaging or fixing.

Antibodies, reagents and cDNA constructs

We used primary antibodies to GFP, p-eEF2 Ser52, vGlut1/2/3, p35, Cyclin-dependent kinase5 (Cdk5), FLAG (see Supplementary Data). Labeling was visualized using anti-rabbit Alexa405, anti-chicken Dylight488, anti-mouse Rhodamine Red-X, anti-guinea pig Alexa647 (Jackson Immunologicals) and anti-sheep Rhodamine (GeneTex). FM4-64

lipophilic dyes were from Molecular Probes, 4EGI-1 from CalBioChem, and Sema3A was from R&D Systems. Mammalian expression constructs that were generated are described in detail in figures and in Supplementary Data. SypHluorin was kindly provided by Yongling Zhu (Salk Institute) (Zhu and Stevens, 2008), and 4E-BP1-4Ala carrying alanine substitutions at four phosphorylation sites (Thr37, Thr46, Ser65, and Thr70), by Dr. Hans G. Wendel (Memorial Sloan-Kettering Cancer Center) (Schatz et al., 2011).

Immunocytochemistry, image acquisition, quantification and analysis

Neurons were fixed with 4% paraformaldehyde, 4% sucrose (wt/vol), permeabilized and blocked in 10% BSA (vol/vol) and 0.2% Triton X-100 (vol/vol), and immunostained at 25 °C for 2 h, or overnight at 4 °C. For quantification of fluorescence intensity, images were acquired on a Zeiss inverted confocal microscope (LSM 780) with a 63× oil-immersion lens and identical laser and gain settings. Images were analyzed using Matlab and ImageJ (NIH). In brief, confocal image stacks (thickness=1.5μm) were average projected into 2D images and imported into SynD (Schmitz et al., 2011). A morphology channel (GFP) was used to generate a mask of transfected axonal or somatodendritic areas. Synaptic vesicle clusters were identified by thresholding and deconvolution of vGlut or FM4-64 labeling (see below) (one standard deviation above the mean vGlut or FM4-64 intensity) within the morphology mask expanded to include 1μm of padding outside the measured neurites. Minimum size for fluorescent clusters was set at 0.35 μm^2. Intensity and area at 50–100 sites were measured in each neuron and averaged; data from several neurons was compared between groups. Data were exported to Excel and statistical analyses were performed using Prism4 (GraphPad). Summary data are reported as mean ± s.e.m. Statistical significance for all quantitation was determined by Student's t test for two samples and by one-way ANOVA for three or more samples unless otherwise specified. Post-tests and p-values are indicated in the relevant figure legends.

Western blots and metabolic labeling

For western blots 293T or Neuro2A cells were seeded and transfected with expression vectors. 24 hours after transfection, cells were lysed in 100μl of RIPA buffer with 1X protease inhibitor cocktail (Roche) and 1mM PMSF, sonicated and nuclei were pelleted. Equal amounts of protein were loaded per lane, resolved by SDS-PAGE, blotted onto PVDF paper, immunolabeled and imaged using LiCor. For metabolic labeling, Met-deprived PC12 cells were incubated with AHA (L-azidohomoalanine); AHA incorporation was evaluated in lysates separated by SDS-PAGE. Labeling in cultured neurons was carried out as described previously (Dieterich et al., 2007; Dieterich et al., 2010).

Detecting endogenous p35 transcripts

Sm-FISH was done as previously described (Raj et al., 2008). Rat p35 probes were designed using Stellaris RNA FISH probe designer, conjugated to Quasar 670, and purified (Biosearch Technologies). DIV 9 cultured rat hippocampal neurons were fixed with paraformaldehyde, and the manufacturer’s protocol was followed as recommended.

Live-cell imaging and fluorescence recovery after photoswitching

Hippocampal neurons (9DIV) plated on 35-mm bottom glass dishes (MatTek) were transfected with mEOS2 cDNA constructs ~16h before imaging. Neurons were switched to pre-equilibrated Hibernate E Low Fluorescence medium (Brain Bits) and experiment was performed using a Zeiss LSM780 inverted confocal microscope fitted with a heated stage similar to previous work (Aakalu et al., 2001; Leung and Holt, 2008; Nie et al., 2010). Axons were optically isolated by photoswitching cell bodies every 2 mins throughout the duration of the experiment (Aakalu et al., 2001). Fluorescence intensity was measured using ImageJ and two-way ANOVA was used to compare signal recovery over the course of 1hr and between reporters.

Time lapse, FM dye and SypHluorin experiments

For growth cone collapse, neurons were seeded on PLL coated glass bottom dishes in phenol red free Neurobasal media supplemented with NS21. Images were acquired before and after 15 – 20 mins Sema3A (200 ng/mL) treatment on Zeiss LSM780 inverted microscope within an environmentally controlled chamber maintained at 37°C, 5% $C0_2$.

FM dye uptake was stimulated by depolarizing buffer (70 mM NaCl, 75 mM KCl, 2 mM $CaCl_2$, 2 mM $MgCl_2$, 5.5 mM glucose and 20 mM HEPES, pH = 7.3) with FM4-64 (x concentration; Invitrogen). AP5 (50 μM) and CNQX (25 μM) were added to prevent recurrent excitation. Neurons were washed in Ca^{2+}-free solution containing ADVASEP-7 (0.1 mM; Sigma) and images were acquired. Labeled sites were analyzed using SynD (see above). For SypHluorin experiments, transfected cells were identified by faint GFP fluorescence under nondepolarizing conditions. Images were collected with 488ex/505em filter sets before and after depolarization in the presence of 1 μM bafilomycin (Tocris) to inhibit the vesicular H^+ ATPase. Vesicle clusters exhibiting lateral movement were excluded from analysis.

RESULTS

Targeting a cap-dependent translation repressor to distal neuronal processes

In order to assess the contribution of intra-axonal translation to synapse development we made a translational repressor that could be expressed at sites remote to the cell body. The translation of most cellular mRNAs is cap-dependent and relies on a translation initiation complex (eIF4F) that includes cap binding protein (eIF4E), an RNA helicase, and a scaffolding protein (eIF4G) that bridges the complex to ribosomes. eIF4E binding proteins (4E-BPs) competitively displace eIF4G, and repress translation. 4E-BP binding to eIF4E is negatively regulated by phosphorylation and this regulatory step can be exploited by exogenous expression of a non-phosphorylatable 4E-BP mutant in which three threonines and one serine have been mutated to alanines (4E-BP1-4A) (Gingras et al., 1999; Rong et al., 2008). Since most translation requires only low levels of eIF4E, this and similar manipulations affect preferentially a set of highly regulated mRNAs, including many of those targeted to distal sites (Gingras et al., 2001; Klann and Dever, 2004; Gkogkas et al., 2013). However, because 4E-BP1-4A is rapidly turned over (Yanagiya et al., 2012) its expression in cell bodies is unlikely to repress distally targeted mRNAs. To circumvent this,

we generated a 4E-BP1-4A mutant encoded by a mRNA transcript having a 3'UTR from β-actin mRNA, which contains a sequence recognized and transported by zipcode-binding protein 1 (ZBP1) into axons and dendrites where it can be translated locally (Kislauskis et al., 1994; Tiruchinapalli et al., 2003); and we placed this fusion gene downstream of an IRES (internal ribosome entry site) in order to escape its own negative regulation (Jang and Wimmer, 1990) (Fig. 1A). We called this mutant, remotely targeted 4E-BP1-4A, or simply "r*em*4A".

Fluorescence-based metabolic labeling (FUNCAT) was used to evaluate total new protein synthesis in PC12 cells expressing *rem*4A. PC12 cells were transfected with an inducible version of *rem*4A (tetOFF4A) and maintained in or withdrawn from doxycycline for 48h, metabolically labeled with AHA (L-azidohomoalanine), a Met-like amino acid, and AHA incorporation was evaluated in lysates separated by SDS-PAGE. As expected *rem*4A expression had little impact on overall levels of new protein synthesis (Graff et al., 2007; Gkogkas et al., 2013) (Fig. 1B). Hypophosphorylation of 4E-BP is usually accompanied by phosphorylation of elongation factor 2 (eEF2) (Liu et al., 2006; Rose et al., 2009), a modification that also represses translation (Ryazanov et al., 1988). Thus, as a proxy for *rem*4A effects, localization of p-eEF2 was evaluated in hippocampal neurons expressing *rem*4A or *dUTR*4A (a non-targeting transcript lacking the 3'UTR; Fig. 1A) as a control. p-eEF2 immunolabeling was enriched at distal as well as in proximal processes in neurons expressing *rem*4A compared to neurons expressing *dUTR*4A, the non-targeting transcript (Fig. 1C, D).

To test whether targeted repression of cap-dependent translation is functionally relevant we took advantage of a well-characterized effect of Sema3A on axonal growth cones. When applied at a low dose, Sema3A promotes a local protein synthesis dependent form of growth cone collapse (Campbell and Holt, 2001; Manns et al., 2012) requiring the generation of rhoA and NF-protocadherin (. Cortical neurons were transiently transfected at 2 DIV with vector alone, *rem*4A, or *dUTR*4A and at 3 DIV growth cones were imaged before and 15 min after exposure to Sema3A. In neurons expressing vector alone, Sema3A provoked collapse in 61% of growth cones similar to previous studies (Carcea et al., 2010). Consistent with a requirement for cap-dependent translation, addition of 4EGI, a small molecule inhibitor of eIF4G binding to eIF4E (Moerke et al., 2007), 20 mins prior to the addition of Sema3A abrogated collapse (12% collapse). Axons expressing *rem*4A showed no collapse (11%) similar to 4EGI, while *dUTR*4A growth cones responded similar to vector expressing controls (52%) (Fig. 1E) (Chi Square, $p<0.001$ for GFP vs. 4EGI or *rem*4A; 50 neurons per group).

That the effect of *rem*4A is due to repression of protein translation is further supported by FUNCAT localization. In *dUTR*4A expressing neurons, Sema3A increased AHA incorporation in growth cones with no change observed in *rem*4A neurons or vehicle-treated controls (Fig. 1F–H). In contrast Sema3A modestly decreased AHA incorporation in cell bodies, but there were no differences between untransfected cell bodies and those expressing *dUTR*4A or *rem*4A (one way ANOVA, $p = 0.22$). Additionally, no differences were detected in FLAG-tagged protein levels generated by the two constructs (data not shown). In adult dorsal root ganglia, ZBP1 levels are very low and can be rate limiting for the transport of β-

actin transcripts (Donnelly et al., 2011). However, limited ZBP1 supply does not appear to be relevant for the transport of *rem*4A here as ZBP1 levels are high in developing hippocampal neurons (Gu et al., 2002; Tiruchinapalli et al., 2003) and F-actin levels are similar between *dUTR*4A and *rem*4A expressing axons (t-test, mean rhodamine phalloidin intensity, $p = 0.4378$). The latter is also consistent with previous work showing that Sema3A-mediated collapse requires local translation of RhoA and NF-protocadherin (Wu et al., 2005; Leung et al., 2013), but occurs independent of local actin translation (Leung et al, 2006). Taken together, the data show that transient expression of a translational repressor interferes with intra-axonal translation machinery and growth cone function and that the strategy is effective only when transcripts encoding the repressor are targeted to remote sites.

Presynaptic translation regulates recycling vesicle pool

To assess whether targeted repression of intra-axonal translation alters vesicle recycling, we generated mosaic cultures in which a small number of neurons expressing either *rem*4A or vector alone were surrounded by a much larger number of untransfected neurons. At 10–12 DIV (18h after transfection), neurons were stimulated with a hyperkalemic solution in the presence of FM4-64, a lipophilic styryl dye used to fluorescently label recycling synaptic vesicles. When vesicles fuse, the compound is incorporated into the exposed internal leaflets, and after endocytosis, the recycled vesicles remain fluorescent (Betz et al., 1996). Area and intensity of recycling vesicle clusters in transfected axons contacting unlabeled dendrites (*cis*) or vice versa (*trans*) (Fig. 2A, B) were measured using a semi-automated approach (Schmitz et al., 2011) (Fig. S1). The data show that presynaptic expression of *rem*4A increased intensity and area of FM-dye labeled sites (Fig. 2C), while postsynaptic expression of *rem*4A exerted no trans-synaptic effect on either the intensity or area of FM-dye labeled sites (Fig. 2D). By contrast, postsynaptic expression of *rem*4A reduced PSD95 intensity (Fig. S1) consistent with previous work showing PSD95 levels can be regulated by local, dendritic translation (Muddashetty et al., 2007).

FM-dyes can modulate vesicle recycling on their own (Zhu and Stevens, 2008). Thus to confirm our findings, neurons were transfected with SypHluorin, a pH sensitive probe that is targeted to the lumenal surface of vesicles and shows increased fluorescence intensity at higher pH (following exocytosis) (Zhu and Stevens, 2008), alone or together with DsRed-*rem*4A. Neurons were imaged and depolarized in the presence of bafilomycin, to prevent vesicle re-acidification, and the change in fluorescence (ΔF) between resting and stimulated status was compared. The data show that ΔF in *rem*4A axons was significantly greater than in controls, consistent with an increase in the vesicle recycling pool (Fig. 2 E, F).

To test whether size of the total pool of vesicles (which includes recycling and reserve pools) is altered, immunolabeling intensity for vesicular glutamate transporters (vGluts)1–3 was compared in neurons expressing *rem*4A or vector alone. There were no significant differences between the groups (mean intensity 547 ± 34 (GFP, n = 11) vs. 525 ± 42 (*rem*4A, n =13), t-test, $p = 0.7$). Taken together the data indicate that targeted repression of cap-dependent translation in axons increases the recycling pool of vesicles without changing

the total pool. This could occur by recruiting vesicles from the reserve pool, but could also reflect changes in vesicle organization and packing.

Cdk5/p35 signaling is regulated by cap-dependent translation

The increased recycling pool size observed in axons expressing *rem*4A resembles effects of cyclin-dependent kinase 5 (Cdk5) inhibition on presynaptic terminals (Tomizawa et al., 2003; Kim and Ryan, 2010). Cdk5 activity is regulated by p35, a protein that can be regulated by degradation (Patrick et al., 1998; Kusakawa et al., 2000; Lee et al., 2000). We asked whether p35 levels are also controlled by cap-dependent translation. To test this, we co-expressed full-length p35 cDNA in HEK cells with or without *rem*4A. Western blots of whole cell lysates show that *rem*4A expression decreased p35 levels and that this effect required an intact 5'UTR; replacing the 5'UTR with an IRES sequence upstream of the p35 coding region rendered p35 protein levels resistant to *rem*4A mediated repression (Fig. 3A, B). To confirm this effect in a more relevant environment, Neuro2A cells were transiently transfected with *rem*4A. While transfection efficiency is less than 100% (~70%), it is higher and far more consistent than in primary neurons so that the impact of *rem*4A on endogenous proteins can be measured biochemically. Western blots show that *rem*4A expression decreased p35 levels compared to expression of vector alone (Fig. 3C, D). Levels of CaMKIIα were also appeared reduced by *rem*4A as expected, although the result failed to reach statistical significance (Burgin et al., 1990; Benson et al., 1992; Aakalu et al., 2001). Levels of a regulatory subunit of PKA, PKARIIβ, were unchanged (Fig. 3C, D).

In neurons, immunolabeling for endogenous p35 extended throughout all processes with greater enrichment in cell bodies and dendrites than in axons, which were identified by labeling for an axonal marker (SMI31, Fig. 3E, F). In both dendrites and axons, immunolabeling was partially punctate. Some p35 puncta colocalized with vGlut-labeled clusters along dendrites, which are presumably synapses (Fig. 3E), but also with vGlut clusters at non-synaptic hot spots in axons having no nearby dendrites (Fig. 3F). To test whether p35 levels at vesicle recycling sites are diminished by *rem*4A, neurons expressing *rem*4A or vector alone were stimulated in the presence of a fixable version of FM dye and then fixed and immunolabeled for p35. At recycling sites in axons expressing *rem*4A, labeling intensity for p35 was significantly diminished relative to control (Fig. 3G).

To test whether p35 levels regulate vesicle recycling, FM dye uptake was stimulated and recycling pools were compared in neurons expressing vector alone, p35 shRNA, or exposed to 4EGI. The data show increased FM dye intensity and area in p35 knockdown axons as well as following bath application of 4EGI (Fig. 3H–J). These data support that the increased recycling pool size observed in *rem*4A expressing axons is due at least in part to decreased presynaptic p35 levels.

Local mRNA translation contributes to axonal p35 levels

Our data suggest that p35 is translated locally in axons. A recent study reported that p35 mRNA is transported into axons (Zivraj et al., 2010); and this was confirmed using single-molecule (sm)-FISH, a fluorescence in situ hybridization method utilizing multiple fluorescent oligonucleotide probes (Raj et al., 2008; Akins et al., 2012; Cajigas et al., 2012).

The greatest density of p35 mRNA labeling was in cell bodies, dendrites showed a decreasing gradient, and axons displayed an irregular distribution pattern with regions of greater and lesser intensity (Fig. 4A–C).

To test whether p35 can be translated locally in axons and dendrites as well as in cell bodies, we generated a p35 translation reporter in which mEOS2, an irreversible photoswitchable tag (McKinney et al., 2009), was flanked by the full length 5' and 3' UTRs of p35 mRNA (p35mEOS2-fL) and a control reporter having a truncated 3'UTR (p35mEOS2-dUTR) (Aakalu et al., 2001; Leung et al., 2006). In both constructs mEOS2 was preceded by the first 16aa of p35, which encodes a myristoylation site (Hisanaga and Saito, 2003), so that the reporter will be anchored to the membrane near its site of synthesis (Aakalu et al., 2001) (Fig. 4D). Neurons were transfected with the reporters at 9 DIV and identified by green fluorescence ~16h later. New protein synthesis in axons was assessed by measuring accumulation of green in axons that had been photoswitched to red and isolated "optically" (Aakalu et al., 2001) to eliminate contributions of newly synthesized green proteins transported from cell bodies. At t = 0, the entire neuron was photoswitched from green (excitation λ = 488 nm, emission λ = 516 nm) to red (561 nm; 581nm) using 405 nm laser light; cell bodies were photoswitched repeatedly every 2 mins throughout the duration of the experiment (Fig. 4F); and appearance of green was monitored in axons every 10 – 20 mins. Recovery of green p35mEOS2-fL fluorescence was detected by 10 mins and continued to increase over 60 mins. Truncating the 3'UTR (p35mEOS2-dUTR) eliminated this effect. (Fig. 4E, G, 2-way ANOVA, $p < .0001$). These data indicate that p35 can be generated locally within axons at sites distant from growth cones.

Intra-axonal translation regulates presynaptic p35 expression

Our data show that p35 levels in axons are decreased by *rem*4A and that p35 knockdown increases vesicle recycling pool size similar to *rem*4A expression (Figs. 3H, 2C). If diminished p35 levels account for the changes in vesicle recycling caused by targeted translational repression in axons, then restoring p35 protein levels by expressing cap-independent IRES-p35 transcripts should rescue the presynaptic phenotype. Using fixable FM dye labeling, we compared vesicle recycling in axons co-expressing IRES-p35 and *rem*4A to those expressing *rem*4A or vector alone. The data show that IRES-p35 expression restores vesicle recycling in axons expressing *rem*4A to control values (Fig. 5A, B). These data strongly support that cap-dependent intra-axonal translation of p35 constrains the size of synaptic vesicle recycling pools.

DISCUSSION

Here we show that axonal repression of cap-dependent translation increases synaptic vesicle recycling pool size in part by impeding the local production of p35. These data join a small group of studies that collectively show that local synthesis of a select group of axonal mRNAs regulates the generation and function of developing synapses. In neurons cultured from Aplysia local presynaptic production of the neuropeptide, sensorin, promotes the generation of synapses (Lyles et al., 2006) and in rat hippocampal neurons, axonal production of β-catenin restrains synaptic vesicle release kinetics at nascent artificial

synapses contacts generated with poly-D-lysine-coated beads (Taylor et al., 2013). In general there is a reduction in vesicle release probability as hippocampal synapses mature (Bolshakov and Siegelbaum, 1995; Chavis and Westbrook, 2001; Branco et al., 2008) suggesting a model in which adhesion mediated recruitment of ribosomes (Chicurel et al., 1998; Gu et al., 2008; Taylor et al., 2013) at developing synapses serves to promote local synthesis of β-catenin and p35 at presynaptic sites as a necessary step in the maturation of synapses (Bamji et al., 2003; Taylor et al., 2013).

Local production of protein at postsynaptic sites has long been known to influence synapse function (Steward and Schuman, 2001), but most experimental manipulations have failed to exclude potential contributions of presynaptic synthesis, leaving open the possibility that translation at pre- and postsynaptic sites differentially impact synapse development and function. New approaches (Deglincerti and Jaffrey, 2012; Taylor et al., 2013), including those described here, provide the means by which pre- and postsynaptic translation can be measured, manipulated and evaluated separately. In light of this, it is significant that only the targeted translation of *rem*4A had functionally relevant effects on distal axon function and new protein synthesis in growth cones (Fig. 1). While this could be due in part to increased *rem*4A mRNA stability compared to *dUTR*4A, we detected no differences in total protein levels generated by the two constructs. By depending on translation, *rem*4A can regulate only those sites having the appropriate machinery, and by extension *rem*4A would be expected to have more restricted effects in neurons over the course of development.

Our data also show that p35 can be generated locally in axons and that its intra-axonal translation contributes to presynaptic terminal function. Cdk5 that has been activated by p35 phosphorylates several presynaptic proteins including munc18, amphiphysin, dynamin, and synapsin all of which are known to regulate vesicle recycling (Tomizawa et al., 2003; Kim and Ryan, 2010; Su and Tsai, 2011). Intriguingly, p35 and β-catenin can interact and Cdk5 can phosphorylate β-catenin (Kwon et al., 2000; Kesavapany et al., 2001) suggesting that the two locally translated presynaptic proteins could be acting cooperatively to limit synaptic vesicle recycling. However, Cdk5 negatively regulates β-catenin interactions with cadherins (Murase et al., 2002) running counter to a simple cooperative model. p35 is regulated transcriptionally (Harada et al., 2001; McEvilly et al., 2002) as well as locally by proteasome-mediated degradation (Patrick et al., 1998) and calpain-mediated cleavage (Kusakawa et al., 2000; Lee et al., 2000). Our findings indicate that p35 levels can also be controlled locally by selective translation in axons. That Cdk5 activity can be controlled by multiple locally regulated mechanisms is consistent with its potency at synapses (Su and Tsai, 2011; Cheung and Ip, 2012) and underscores the importance of differentiating pre- and postsynaptic effects. It will be important in future experiments to determine whether intra-axonal production of proteins will be relevant to synaptic vesicle recycling in mature axons, when translational machinery is scarce in axons (Bassell et al., 1994), or whether it is invoked by traumatic events and/or by borrowing machinery from other cells (Zheng et al., 2001; Court et al., 2008).

Supplementary Material

Refer to Web version on PubMed Central for supplementary material.

Acknowledgments

The authors would like to acknowledge Roxana Mesias for generating the primary neuronal cultures and our funding sources: Seaver Foundation and NIMH (OB); Simons Foundation and NIMH (DLB).

REFERENCES

Aakalu G, Smith WB, Nguyen N, Jiang C, Schuman EM. Dynamic visualization of local protein synthesis in hippocampal neurons. Neuron. 2001; 30:489–502. [PubMed: 11395009]

Akins MR, Leblanc HF, Stackpole EE, Chyung E, Fallon JR. Systematic mapping of Fragile X granules in the developing mouse brain reveals a potential role for presynaptic FMRP in sensorimotor functions. J Comp Neurol. 2012

Bamji SX, Shimazu K, Kimes N, Huelsken J, Birchmeier W, Lu B, Reichardt LF. Role of beta-catenin in synaptic vesicle localization and presynaptic assembly. Neuron. 2003; 40:719–731. [PubMed: 14622577]

Bassell GJ, Singer RH, Kosik KS. Association of poly(A) mRNA with microtubules in cultured neurons. Neuron. 1994; 12:571–582. [PubMed: 8155320]

Benson DL, Gall CM, Isackson PJ. Dendritic localization of type II calcium calmodulin-dependent protein kinase mRNA in normal and reinnervated rat hippocampus. Neuroscience. 1992; 46:851–857. [PubMed: 1311815]

Betz WJ, Mao F, Smith CB. Imaging exocytosis and endocytosis. Curr Opin Neurobiol. 1996; 6:365–371. [PubMed: 8794083]

Bolshakov VY, Siegelbaum SA. Regulation of hippocampal transmitter release during development and long-term potentiation. Science. 1995; 269:1730–1734. [PubMed: 7569903]

Branco T, Staras K, Darcy KJ, Goda Y. Local dendritic activity sets release probability at hippocampal synapses. Neuron. 2008; 59:475–485. [PubMed: 18701072]

Brittis PA, Lu Q, Flanagan JG. Axonal protein synthesis provides a mechanism for localized regulation at an intermediate target. Cell. 2002; 110:223–235. [PubMed: 12150930]

Burgin KE, Washam MN, Rickling S, Westgate SA, Mobley WC, Kelly PT. *In situ* hybridization histochemistry of Ca++/calmodulin-dependent protein kinase in developing rat brain. J. Neurosci. 1990; 10:1788–1798. [PubMed: 2162385]

Burton SD, Johnson JW, Zeringue HC, Meriney SD. Distinct roles of neuroligin-1 and SynCAM1 in synapse formation and function in primary hippocampal neuronal cultures. Neuroscience. 2012; 215:1–16. [PubMed: 22542674]

Cajigas IJ, Tushev G, Will TJ, tom Dieck S, Fuerst N, Schuman EM. The local transcriptome in the synaptic neuropil revealed by deep sequencing and high-resolution imaging. Neuron. 2012; 74:453–466. [PubMed: 22578497]

Campbell DS, Holt CE. Chemotropic responses of retinal growth cones mediated by rapid local protein synthesis and degradation. Neuron. 2001; 32:1013–1026. [PubMed: 11754834]

Carcea I, Ma'ayan A, Mesias R, Sepulveda B, Salton SR, Benson DL. Flotillin-mediated endocytic events dictate cell type-specific responses to semaphorin 3A. J Neurosci. 2010; 30:15317–15329. [PubMed: 21068336]

Chavis P, Westbrook G. Integrins mediate functional pre- and postsynaptic maturation at a hippocampal synapse. Nature. 2001; 411:317–321. [PubMed: 11357135]

Chen Y, Stevens B, Chang J, Milbrandt J, Barres BA, Hell JW. NS21: re-defined and modified supplement B27 for neuronal cultures. J Neurosci Methods. 2008; 171:239–247. [PubMed: 18471889]

Cheung ZH, Ip NY. Cdk5: a multifaceted kinase in neurodegenerative diseases. Trends Cell Biol. 2012; 22:169–175. [PubMed: 22189166]

Chicurel ME, Singer RH, Meyer CJ, Ingber DE. Integrin binding and mechanical tension induce movement of mRNA and ribosomes to focal adhesions. Nature. 1998; 392:730–733. [PubMed: 9565036]

Christie SB, Akins MR, Schwob JE, Fallon JR. The FXG: a presynaptic fragile X granule expressed in a subset of developing brain circuits. J Neurosci. 2009; 29:1514–1524. [PubMed: 19193898]

Court FA, Hendriks WT, MacGillavry HD, Alvarez J, van Minnen J. Schwann cell to axon transfer of ribosomes: toward a novel understanding of the role of glia in the nervous system. J Neurosci. 2008; 28:11024–11029. [PubMed: 18945910]

Cox LJ, Hengst U, Gurskaya NG, Lukyanov KA, Jaffrey SR. Intra-axonal translation and retrograde trafficking of CREB promotes neuronal survival. Nat Cell Biol. 2008; 10:149–159. [PubMed: 18193038]

Deglincerti A, Jaffrey SR. Insights into the roles of local translation from the axonal transcriptome. Open Biol. 2012; 2:120079. [PubMed: 22773949]

Dieterich DC, Hodas JJ, Gouzer G, Shadrin IY, Ngo JT, Triller A, Tirrell DA, Schuman EM. In situ visualization and dynamics of newly synthesized proteins in rat hippocampal neurons. Nat Neurosci. 2010; 13:897–905. [PubMed: 20543841]

Dieterich DC, Lee JJ, Link AJ, Graumann J, Tirrell DA, Schuman EM. Labeling, detection and identification of newly synthesized proteomes with bioorthogonal non-canonical amino-acid tagging. Nat Protoc. 2007; 2:532–540. [PubMed: 17406607]

Donnelly CJ, Willis DE, Xu M, Tep C, Jiang C, Yoo S, Schanen NC, Kirn-Safran CB, van Minnen J, English A, Yoon SO, Bassell GJ, Twiss JL. Limited availability of ZBP1 restricts axonal mRNA localization and nerve regeneration capacity. EMBO J. 2011; 30:4665–4677. [PubMed: 21964071]

Gingras AC, Gygi SP, Raught B, Polakiewicz RD, Abraham RT, Hoekstra MF, Aebersold R, Sonenberg N. Regulation of 4E-BP1 phosphorylation: a novel two-step mechanism. Genes Dev. 1999; 13:1422–1437. [PubMed: 10364159]

Gingras AC, Raught B, Gygi SP, Niedzwiecka A, Miron M, Burley SK, Polakiewicz RD, Wyslouch-Cieszynska A, Aebersold R, Sonenberg N. Hierarchical phosphorylation of the translation inhibitor 4E-BP1. Genes Dev. 2001; 15:2852–2864. [PubMed: 11691836]

Gkogkas CG, Khoutorsky A, Ran I, Rampakakis E, Nevarko T, Weatherill DB, Vasuta C, Yee S, Truitt M, Dallaire P, Major F, Lasko P, Ruggero D, Nader K, Lacaille JC, Sonenberg N. Autism-related deficits via dysregulated eIF4E-dependent translational control. Nature. 2013; 493:371–377. [PubMed: 23172145]

Graff JR, Konicek BW, Vincent TM, Lynch RL, Monteith D, Weir SN, Schwier P, Capen A, Goode RL, Dowless MS, Chen Y, Zhang H, Sissons S, Cox K, McNulty AM, Parsons SH, Wang T, Sams L, Geeganage S, Douglass LE, Neubauer BL, Dean NM, Blanchard K, Shou J, Stancato LF, Carter JH, Marcusson EG. Therapeutic suppression of translation initiation factor eIF4E expression reduces tumor growth without toxicity. J Clin Invest. 2007; 117:2638–2648. [PubMed: 17786246]

Gu W, Pan F, Zhang H, Bassell GJ, Singer RH. A predominantly nuclear protein affecting cytoplasmic localization of beta-actin mRNA in fibroblasts and neurons. J Cell Biol. 2002; 156:41–51. [PubMed: 11781334]

Gu W, Wells AL, Pan F, Singer RH. Feedback regulation between zipcode binding protein 1 and beta-catenin mRNAs in breast cancer cells. Mol Cell Biol. 2008; 28:4963–4974. [PubMed: 18490442]

Harada T, Morooka T, Ogawa S, Nishida E. ERK induces p35, a neuron-specific activator of Cdk5, through induction of Egr1. Nat Cell Biol. 2001; 3:453–459. [PubMed: 11331872]

Hisanaga S, Saito T. The regulation of cyclin-dependent kinase 5 activity through the metabolism of p35 or p39 Cdk5 activator. Neurosignals. 2003; 12:221–229. [PubMed: 14673209]

Jang SK, Wimmer E. Cap-independent translation of encephalomyocarditis virus RNA: structural elements of the internal ribosomal entry site and involvement of a cellular 57-kD RNA-binding protein. Genes Dev. 1990; 4:1560–1572. [PubMed: 2174810]

Jung H, Yoon BC, Holt CE. Axonal mRNA localization and local protein synthesis in nervous system assembly, maintenance and repair. Nat Rev Neurosci. 2012; 13:308–324. [PubMed: 22498899]

Kesavapany S, Lau KF, McLoughlin DM, Brownlees J, Ackerley S, Leigh PN, Shaw CE, Miller CC. p35/cdk5 binds and phosphorylates beta-catenin and regulates beta-catenin/presenilin-1 interaction. Eur J Neurosci. 2001; 13:241–247. [PubMed: 11168528]

Kim SH, Ryan TA. CDK5 serves as a major control point in neurotransmitter release. Neuron. 2010; 67:797–809. [PubMed: 20826311]

Kislauskis EH, Zhu X, Singer RH. Sequences responsible for intracellular localization of beta-actin messenger RNA also affect cell phenotype. J Cell Biol. 1994; 127:441–451. [PubMed: 7929587]

Klann E, Dever TE. Biochemical mechanisms for translational regulation in synaptic plasticity. Nat Rev Neurosci. 2004; 5:931–942. [PubMed: 15550948]

Kundel M, Jones KJ, Shin CY, Wells DG. Cytoplasmic polyadenylation element-binding protein regulates neurotrophin-3-dependent beta-catenin mRNA translation in developing hippocampal neurons. J Neurosci. 2009; 29:13630–13639. [PubMed: 19864575]

Kusakawa G, Saito T, Onuki R, Ishiguro K, Kishimoto T, Hisanaga S. Calpain-dependent proteolytic cleavage of the p35 cyclin-dependent kinase 5 activator to p25. J Biol Chem. 2000; 275:17166–17172. [PubMed: 10748088]

Kwon YT, Gupta A, Zhou Y, Nikolic M, Tsai LH. Regulation of N-cadherin-mediated adhesion by the p35-Cdk5 kinase. Curr Biol. 2000; 10:363–372. [PubMed: 10753743]

Lee MS, Kwon YT, Li M, Peng J, Friedlander RM, Tsai LH. Neurotoxicity induces cleavage of p35 to p25 by calpain. Nature. 2000; 405:360–364. [PubMed: 10830966]

Leung KM, Holt CE. Live visualization of protein synthesis in axonal growth cones by microinjection of photoconvertible Kaede into Xenopus embryos. Nat Protoc. 2008; 3:1318–1327. [PubMed: 18714300]

Leung KM, van Horck FP, Lin AC, Allison R, Standart N, Holt CE. Asymmetrical beta-actin mRNA translation in growth cones mediates attractive turning to netrin-1. Nat Neurosci. 2006; 9:1247–1256. [PubMed: 16980963]

Leung LC, Urbancic V, Baudet ML, Dwivedy A, Bayley TG, Lee AC, Harris WA, Holt CE. Coupling of NF-protocadherin signaling to axon guidance by cue-induced translation. Nat Neurosci. 2013; 16:166–173. [PubMed: 23292679]

Liu L, Cash TP, Jones RG, Keith B, Thompson CB, Simon MC. Hypoxia-induced energy stress regulates mRNA translation and cell growth. Mol Cell. 2006; 21:521–531. [PubMed: 16483933]

Lyles V, Zhao Y, Martin KC. Synapse formation and mRNA localization in cultured Aplysia neurons. Neuron. 2006; 49:349–356. [PubMed: 16446139]

Manns RP, Cook GM, Holt CE, Keynes RJ. Differing semaphorin 3A concentrations trigger distinct signaling mechanisms in growth cone collapse. J Neurosci. 2012; 32:8554–8559. [PubMed: 22723695]

McEvilly RJ, de Diaz MO, Schonemann MD, Hooshmand F, Rosenfeld MG. Transcriptional regulation of cortical neuron migration by POU domain factors. Science. 2002; 295:1528–1532. [PubMed: 11859196]

McKinney SA, Murphy CS, Hazelwood KL, Davidson MW, Looger LL. A bright and photostable photoconvertible fluorescent protein. Nat Methods. 2009; 6:131–133. [PubMed: 19169260]

Merianda TT, Lin AC, Lam JS, Vuppalanchi D, Willis DE, Karin N, Holt CE, Twiss JL. A functional equivalent of endoplasmic reticulum and Golgi in axons for secretion of locally synthesized proteins. Mol Cell Neurosci. 2009; 40:128–142. [PubMed: 19022387]

Moerke NJ, Aktas H, Chen H, Cantel S, Reibarkh MY, Fahmy A, Gross JD, Degterev A, Yuan J, Chorev M, Halperin JA, Wagner G. Small-molecule inhibition of the interaction between the translation initiation factors eIF4E and eIF4G. Cell. 2007; 128:257–267. [PubMed: 17254965]

Muddashetty RS, Kelic S, Gross C, Xu M, Bassell GJ. Dysregulated metabotropic glutamate receptor-dependent translation of AMPA receptor and postsynaptic density-95 mRNAs at synapses in a mouse model of fragile X syndrome. J Neurosci. 2007; 27:5338–5348. [PubMed: 17507556]

Murase S, Mosser E, Schuman EM. Depolarization drives beta-Catenin into neuronal spines promoting changes in synaptic structure and function. Neuron. 2002; 35:91–105. [PubMed: 12123611]

Nie D, Di Nardo A, Han JM, Baharanyi H, Kramvis I, Huynh T, Dabora S, Codeluppi S, Pandolfi PP, Pasquale EB, Sahin M. Tsc2-Rheb signaling regulates EphA-mediated axon guidance. Nat Neurosci. 2010; 13:163–172. [PubMed: 20062052]

Patrick GN, Zhou P, Kwon YT, Howley PM, Tsai LH. p35, the neuronal-specific activator of cyclin-dependent kinase 5 (Cdk5) is degraded by the ubiquitin-proteasome pathway. J Biol Chem. 1998; 273:24057–24064. [PubMed: 9727024]

Perry RB, Doron-Mandel E, Iavnilovitch E, Rishal I, Dagan SY, Tsoory M, Coppola G, McDonald MK, Gomes C, Geschwind DH, Twiss JL, Yaron A, Fainzilber M. Subcellular knockout of importin beta1 perturbs axonal retrograde signaling. Neuron. 2012; 75:294–305. [PubMed: 22841314]

Poon MM, Choi SH, Jamieson CA, Geschwind DH, Martin KC. Identification of process-localized mRNAs from cultured rodent hippocampal neurons. J Neurosci. 2006; 26:13390–13399. [PubMed: 17182790]

Raj A, van den Bogaard P, Rifkin SA, van Oudenaarden A, Tyagi S. Imaging individual mRNA molecules using multiple singly labeled probes. Nat Methods. 2008; 5:877–879. [PubMed: 18806792]

Rong L, Livingstone M, Sukarieh R, Petroulakis E, Gingras AC, Crosby K, Smith B, Polakiewicz RD, Pelletier J, Ferraiuolo MA, Sonenberg N. Control of eIF4E cellular localization by eIF4E-binding proteins, 4E-BPs. RNA. 2008; 14:1318–1327. [PubMed: 18515545]

Rose AJ, Bisiani B, Vistisen B, Kiens B, Richter EA. Skeletal muscle eEF2 and 4EBP1 phosphorylation during endurance exercise is dependent on intensity and muscle fiber type. Am J Physiol Regul Integr Comp Physiol. 2009; 296:R326–R333. [PubMed: 19036825]

Ryazanov AG, Shestakova EA, Natapov PG. Phosphorylation of elongation factor 2 by EF-2 kinase affects rate of translation. Nature. 1988; 334:170–173. [PubMed: 3386756]

Schatz JH, Oricchio E, Wolfe AL, Jiang M, Linkov I, Maragulia J, Shi W, Zhang Z, Rajasekhar VK, Pagano NC, Porco JA Jr, Teruya-Feldstein J, Rosen N, Zelenetz AD, Pelletier J, Wendel HG. Targeting cap-dependent translation blocks converging survival signals by AKT and PIM kinases in lymphoma. J Exp Med. 2011; 208:1799–1807. [PubMed: 21859846]

Schmitz SK, Hjorth JJ, Joemai RM, Wijntjes R, Eijgenraam S, de Bruijn P, Georgiou C, de Jong AP, van Ooyen A, Verhage M, Cornelisse LN, Toonen RF, Veldkamp WJ. Automated analysis of neuronal morphology, synapse number and synaptic recruitment. J Neurosci Methods. 2011; 195:185–193. [PubMed: 21167201]

Steward O, Schuman EM. Protein synthesis at synaptic sites on dendrites. Annu Rev Neurosci. 2001; 24:299–325. [PubMed: 11283313]

Su SC, Tsai LH. Cyclin-dependent kinases in brain development and disease. Annu Rev Cell Dev Biol. 2011; 27:465–491. [PubMed: 21740229]

Taylor AM, Berchtold NC, Perreau VM, Tu CH, Li Jeon N, Cotman CW. Axonal mRNA in uninjured and regenerating cortical mammalian axons. J Neurosci. 2009; 29:4697–4707. [PubMed: 19369540]

Taylor AM, Wu J, Tai HC, Schuman EM. Axonal translation of beta-catenin regulates synaptic vesicle dynamics. J Neurosci. 2013; 33:5584–5589. [PubMed: 23536073]

Tiruchinapalli DM, Oleynikov Y, Kelic S, Shenoy SM, Hartley A, Stanton PK, Singer RH, Bassell GJ. Activity-dependent trafficking and dynamic localization of zipcode binding protein 1 and beta-actin mRNA in dendrites and spines of hippocampal neurons. J Neurosci. 2003; 23:3251–3261. [PubMed: 12716932]

Tomizawa K, Sunada S, Lu YF, Oda Y, Kinuta M, Ohshima T, Saito T, Wei FY, Matsushita M, Li ST, Tsutsui K, Hisanaga S, Mikoshiba K, Takei K, Matsui H. Cophosphorylation of amphiphysin I and dynamin I by Cdk5 regulates clathrin-mediated endocytosis of synaptic vesicles. J Cell Biol. 2003; 163:813–824. [PubMed: 14623869]

Vogelaar CF, Gervasi NM, Gumy LF, Story DJ, Raha-Chowdhury R, Leung KM, Holt CE, Fawcett JW. Axonal mRNAs: characterisation and role in the growth and regeneration of dorsal root ganglion axons and growth cones. Mol Cell Neurosci. 2009; 42:102–115. [PubMed: 19520167]

Wu KY, Hengst U, Cox LJ, Macosko EZ, Jeromin A, Urquhart ER, Jaffrey SR. Local translation of RhoA regulates growth cone collapse. Nature. 2005; 436:1020–1024. [PubMed: 16107849]

Yanagiya A, Suyama E, Adachi H, Svitkin YV, Aza-Blanc P, Imataka H, Mikami S, Martineau Y, Ronai ZA, Sonenberg N. Translational homeostasis via the mRNA cap-binding protein, eIF4E. Mol Cell. 2012; 46:847–858. [PubMed: 22578813]

Yao J, Sasaki Y, Wen Z, Bassell GJ, Zheng JQ. An essential role for beta-actin mRNA localization and translation in Ca2+-dependent growth cone guidance. Nat Neurosci. 2006; 9:1265–1273. [PubMed: 16980965]

Zhang X, Poo MM. Localized synaptic potentiation by BDNF requires local protein synthesis in the developing axon. Neuron. 2002; 36:675–688. [PubMed: 12441056]

Zheng JQ, Kelly TK, Chang B, Ryazantsev S, Rajasekaran AK, Martin KC, Twiss JL. A functional role for intra-axonal protein synthesis during axonal regeneration from adult sensory neurons. J Neurosci. 2001; 21:9291–9303. [PubMed: 11717363]

Zhu Y, Stevens CF. Probing synaptic vesicle fusion by altering mechanical properties of the neuronal surface membrane. Proc Natl Acad Sci U S A. 2008; 105:18018–18022. [PubMed: 19004790]

Zivraj KH, Tung YC, Piper M, Gumy L, Fawcett JW, Yeo GS, Holt CE. Subcellular profiling reveals distinct and developmentally regulated repertoire of growth cone mRNAs. J Neurosci. 2010; 30:15464–15478. [PubMed: 21084603]

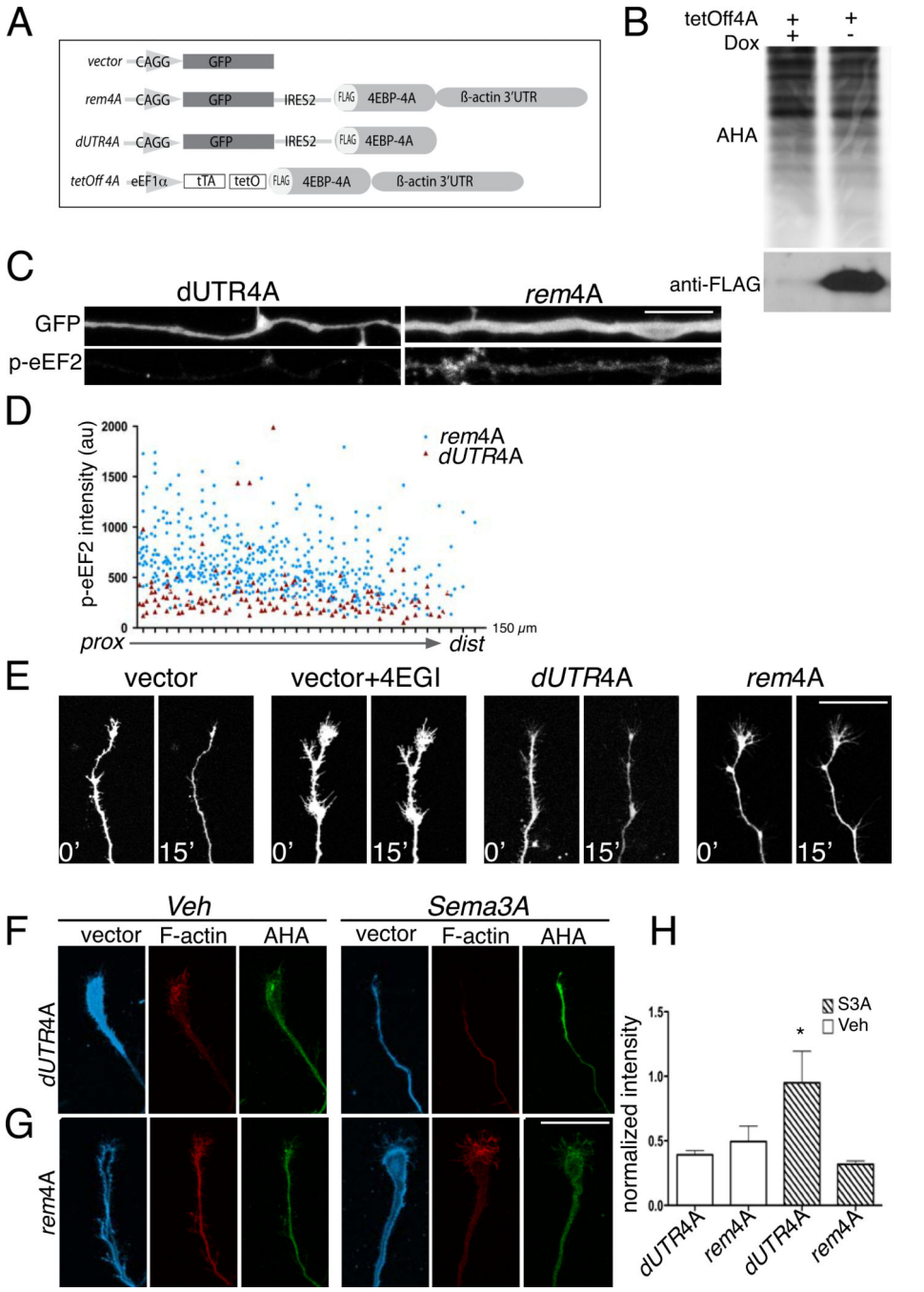

Figure 1. Development and characterization of a targeted translation repressor

Schematic diagrams (A) illustrate the basic domain organization and features of *rem*4A and control vectors. PC12 cells (B) were transfected with tetOFF *rem*4A and the effect of 48h doxycycline (Dox) withdrawal was tested using AHA (L-azidohomoalaine) incorporation followed by a click chemistry reaction using azide-reactive Seta-650-DBCO. Cells were solubilized and run on 12% SDS PAGE and visualized using 680nm channel in Licor before transfer to PVDF membrane and blot against FLAG-tag to detect rem4A expression. Confocal images (C) show axons from cultured hippocampal neurons expressing *dUTR*4A

or *rem*4A that were immunostained for GFP and p-eEF2. Processes were straightened using Image J. (D) Intensity measurements along the lengths of neuronal processes (excluding cell bodies) were binned. Neurons expressing *rem*4A (blue) show higher p-eEF2 intensity than those expressing *dUTR*4A (brown) and levels remain higher distally. (E) Confocal image pairs are of the same axon expressing the constructs indicated in headings and imaged before (0') and after application of Sema3A (15'). Collapse response seen in axons expressing vector only is prevented by 4EGI or *rem*4A, but not by *dUTR*4A (values provided in text). Consistent with these functional data, confocal images (F, G) show AHA-Met incorporation (green) is enhanced by Sema3A exposure in neurons expressing *dUTR*4A relative to vehicle (F), but not in growth cones expressing *rem*4A (G). GFP fluorescence from transfected neurons is shown in blue. Growth cone morphology and collapse response to Sema3A is shown with Texas red phalloidin labeling (red). (H) Bar graph shows relative increase in AHA labeling intensity following Sema3A exposure in growth cones expressing dUTR4A (*$p < 0.05$, one way ANOVA). Mag bars = 50 μm in E, F, G; 15.5 μm in C.

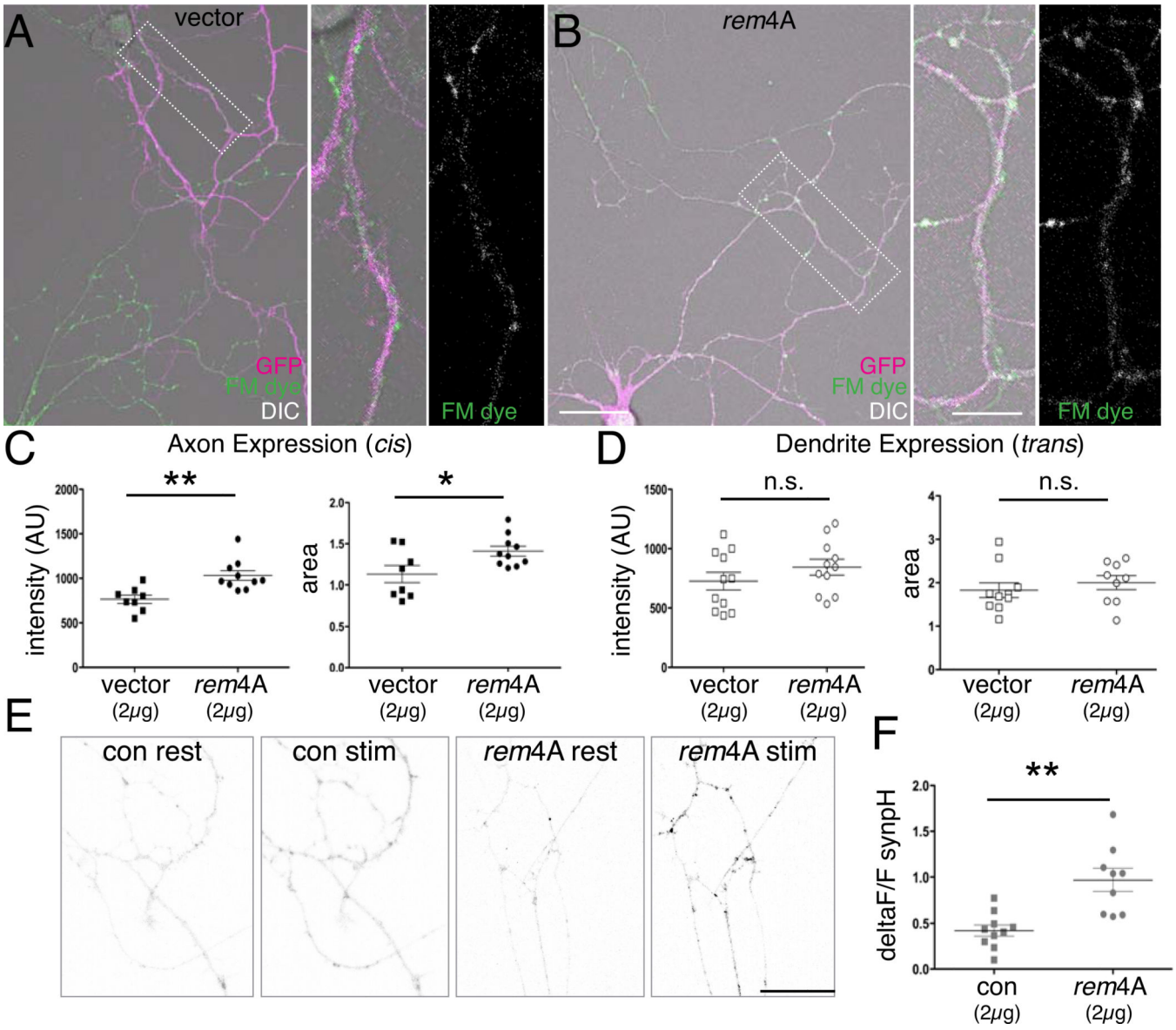

Figure 2. rem4A alters presynaptic function in cis

Confocal images in (A) and (B) illustrate the preparations used to evaluate FM dye uptake (shown in green in color overlays or in white) in living axons transfected with vector only (A) or *rem*4A (B). GFP labeling from transfected neurons is shown in magenta together with DIC image of neurons. Boxed areas are shown at higher mag to the right of each image, first as a color overlay and then with FM dye in gray scale so that labeling can be seen clearly. Scatterplots (C, D) show changes in recycling site intensity and area at sites expressing the construct in *cis* (in axons; C) or in *trans* (in dendrites; D). Confocal image pairs in E show neurons transfected with SypHluorin alone (con) or together with DsRed-*rem*4A (rem4A) as indicated, before (rest) and after stimulation (stim) in the presence of bafilomycin. Data are summarized in F. *$p < 0.05$; ** $p = 0.002$, unpaired two-tailed t-tests. Numbers in μg beneath x-axis labels indicate the amount of cDNA construct transfected. Mag bars = 30 and 15 μm (enlargement) in A, B; 30 μm, E.

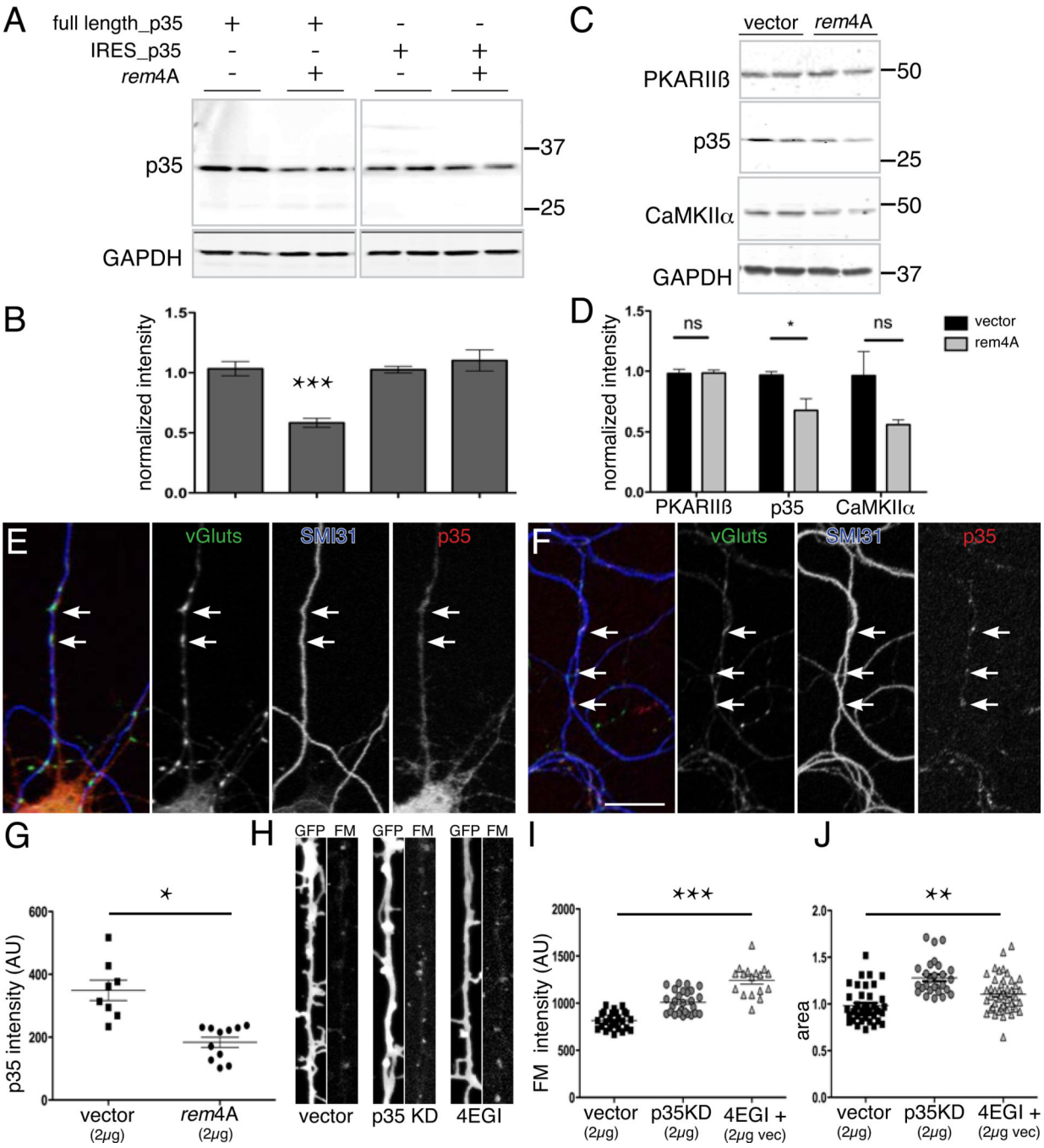

Figure 3. p35 is regulated by cap-dependent translation

(A) HEK cells were transfected with the constructs indicated and then immunoblotted for p35 and GAPDH (as a loading control). Data were visualized and documented using a LiCor (examples shown are taken from the same blot). Numbers at right and in C are molecular weights of size standards (in kDa) (B) Bar graph of p35 intensity normalized to loading control. One way ANOVA, p = .0001, Tukey's post test, ***p = 0.0001, compared to all other conditions. Examples of western blots of lysates from Neuro2A cells expressing the constructs indicated in the headings (C) and then blotted for the antibodies listed. (D) Bar

graph shows quantification of western blot data normalized to loading control (*p = 0.04, t-test). Confocal images (E, F) show endogenous p35 immunolabeling (red in overlay) in the context of vGlut (green in overlay) and SMI31 labeling for axons (blue in overlay) at sites of axodendritic contact (E) or in free axons having no contacts (F). Arrows indicate colocalized clusters of vGlut or p35 labeling. Scatter plots (G) show significantly decreased p35 immunolabeling in masks defined by FM dye uptake in axons transfected with GFP vs. *rem*4A (strategy as in Supplementary Fig. 1). Pairs of confocal images (H) show examples of axons transfected (GFP, left) with the indicated constructs (written below each pair) and then loaded with FM dye (right); processes were straightened using an Image J plugin. Scatter plots compare FM dye labeling intensity (I) and area (J). One way ANOVA $p < .001$; Tukey's post-test ***p<.001, **p<.01 all groups compared to vector. Numbers in μg beneath x-axis labels indicate the amount of cDNA construct transfected. Mag bar = 15 μm.

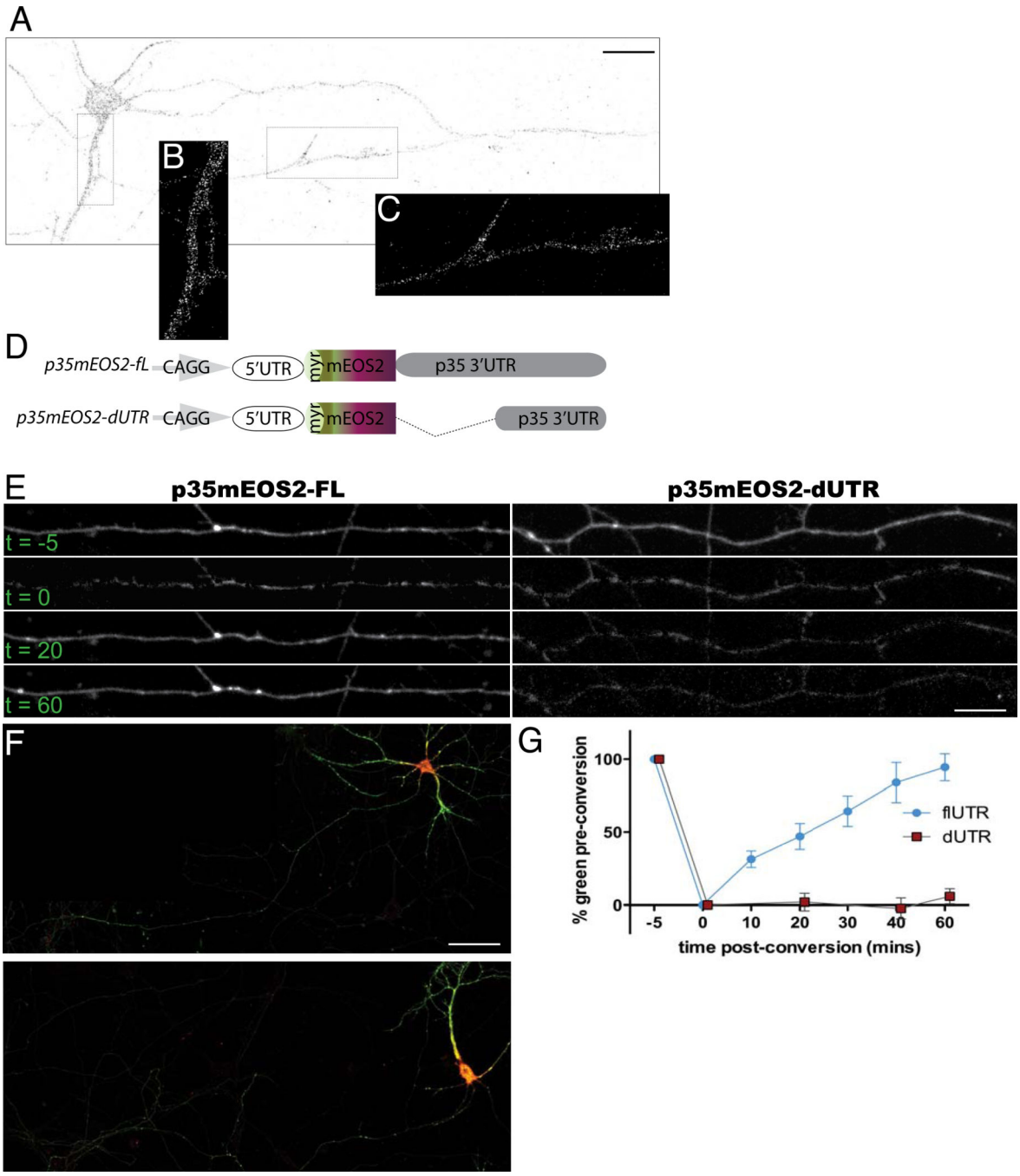

Figure 4. Intra-axonal de novo synthesis of p35

(A) Inverted confocal image of sm-FISH labeling for p35 mRNA in a cultured neuron. Fluorescent clusters, probably indicative of mRNA granules, are observed in dendrites (B, enlargement of region in A) and axons (C, enlargement of region in A). (D) Cartoons show p35 translation reporters driven by pCAGG promoter and flanked by p35 5'UTR and either full length or truncated p35 3'UTR. Photoswitchable mEOS2 is preceded by the first 16 aa of p35, which contains a myristoylation sequence (Myr). p35 translation reporters were introduced at 9DIV and images were taken ~16 hours later with green filter (E, F) and red

filter (F and not shown). At t = 0, green fluorescence in the entire neuron was photoswitched to red and accumulation of green was then monitored in axons at the indicated times (E and G). Cell bodies were photoswitched every 2 mins throughout the duration of the experiment to exclude contributions from this source (as in F). 2-way ANOVA of construct vs. time (G), $p < .0001$; Mag bars = 14 μm (A) and 7 μm (B, C, E), and 65 μm (E, F).

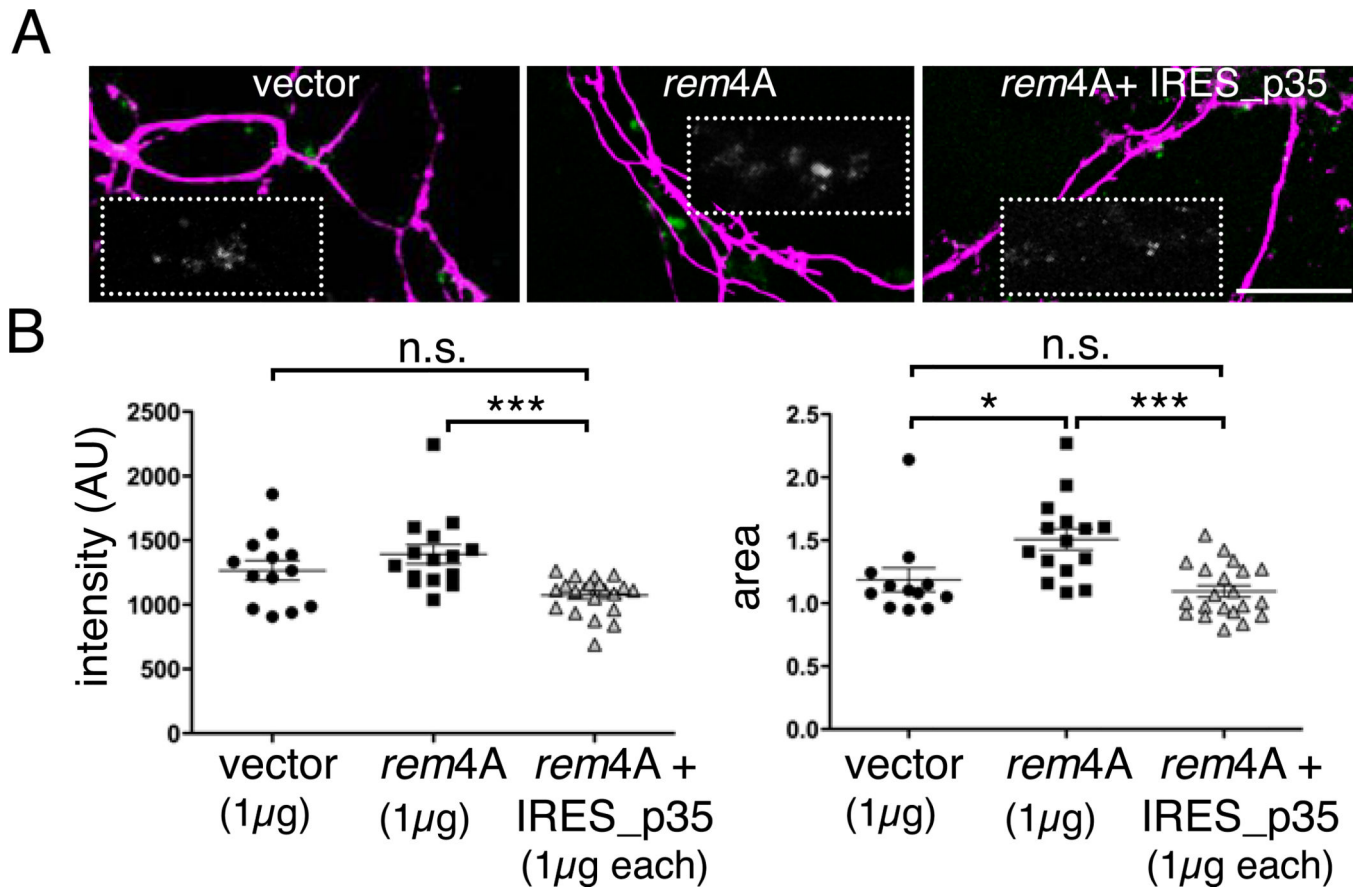

Figure 5. IRES driven p35 expression restores synaptic vesicle recycling in translation-repressed axons

Confocal images (A) and scatter plots (B) compare vector and *rem*4A expressed alone and together with IRES-p35 in axons of 9 DIV neurons. 1-way ANOVA, p = .003 (area) and . 007 (intensity), Tukey's post hoc test, *p<.05; ***p<.001; n.s. is not significant). Mean intensity increase observed with *rem*4A alone is less than (B) what was observed in Fig 2C likely because the amount of *rem*4A cDNA transfected was reduced by 50% (1μg here vs. 2μg in Fig 2) in order to permit co-transfection with IRES-p35 cDNA. Numbers in μg beneath x-axis labels indicate the amount of cDNA construct transfected. Mag bar = 16 μm.